A signal processing method to improve the detection accuracy of co gas concentration in TDLAS detection

12: A SIGNAL PROCESSING METHOD TO IMPROVE THE DETECTION ACCURACY OF CO GAS CONCENTRATION IN TDLAS DETECTION

Yingshuai Li[a]*,Guangdi Mao*[b]*,Qiaofeng Yi*[b]*,Jie Hu*[b]*,Hongmin Zhang*[b]*,Yanong Ning*[b]*,Tongyu Liu*[a,b,*]

[a] Laser Institute, Qilu University of Technology (Shandong Academy of Sciences), Jinan Shandong, China, 250104:
[b] Shandong Micro-sensor Photonics Co. Ltd, Jinan Shandong, China, 250103:

Spectroscopy, EM010, August 12, 2024, 11:30 AM - 12:40 PM

Abstract – This paper presents a signal processing scheme that can suppressing background noise arising from laser-induced interference within the detection signal in a tunable diode laser absorption spectroscopy (TDLAS). The constraints imposed on high-precision gas detection in the system by interference fringes were discussed, with particular emphasis on investigating the mechanisms underlying interference fringe generation. In this scheme, the detected signal was processed with a number of "steps" in order to remove part of the signal variation caused by the interference in the TDLAS system. A test set up was used to verify the scheme. The experimental results demonstrate that this algorithm enhances the stability of gas detection. The dispersion of carbon monoxide concentration values decreased by 24.3%. Moreover, this algorithm exclusively addresses the inherent interference noise floor from the laser, and it can be integrated with algorithms aimed at suppressing other interference fringes, thereby enhancing its denoising capability.

Keywords**:** gas detection; TDLAS; interference noise; signal processing

1. INTRODUCTION

The concentration of CO gas stands as one of the paramount parameters in preventing and managing spontaneous combustion within coal mine goafs[1]. By monitoring trace variations in carbon monoxide composition within coal mines, it becomes feasible to assess the potential hazards for spontaneous combustion; therefore, continually enhancing the concentration detection accuracy of carbon monoxide sensors is imperative. Currently, conventional methods for measuring gas concentration typically involve utilizing the physical and chemical properties of the gases to be monitored, traditional gas detection methods encompass techniques such as potentiometric electrolysis, catalytic combustion, and gas chromatography, among other non-spectroscopic analytical approaches. While these methods offer advantages such as low cost and simplicity in measurement principles, they require frequent calibration to minimize false alarms. Additionally, sensors of this kind are susceptible to corrosion damage in the harsh underground environment of mines, exhibiting poor real-time capabilities and intelligence. With the continuous advancement of the semiconductor laser industry, Tunable Diode Laser Absorption Spectroscopy (TDLAS) technology, renowned for its high sensitivity, excellent selectivity, and rapid response time, has found wide-ranging applications in gas concentration detection and related fields[2]. It is well-known that the fundamental principle of TDLAS technology relies on the Lambert-Beer Law, utilizing the distinct spectral absorption characteristics of various gases for concentration measurements. In a TDLAS system, the laser beam emitted by the laser diode traverses through the gas medium, the output wavelength of the laser diode is tuned with a saw-tooth wave current, when the tuned wavelength aligns with the absorption peak wavelength of the gas, the energy of the laser beam will be absorbed by the gas absorption peak, resulting in attenuation of energy at that wavelength. With the interaction length between the measured gas and the laser beam being fixed in the sensing chamber, by measuring the relative attenuation of light intensity at that wavelength at a photo detector that receives the laser beam. After the calibration, the relationship between gas concentration and the detected light beam intensity can be established. Subsequently, the concentration of the measured gas can be inferred through inversion formulas. Currently, in TDLAS measurement technology, commonly employed detection methods include direct absorption, wavelength-tuned differential absorption detection, and wavelength modulation harmonic detection. The direct absorption method utilizes the detected changes in light intensity to infer the gas concentration, while the wavelength-tuned differential absorption detection relies on the difference in optical intensities between the absorption spectral signals and non-absorption spectral signal to estimate gas concentration. The wavelength modulation harmonic detection, on the other hand, involves analyzing and calculating gas concentration through the analysis of the second harmonic signal using a lock-in amplifier. As TDLAS technology fundamentally involves the detection and processing of analog signals, it constitutes a linear measurement process. Therefore, various interference noise signals generated by the sensor detection system can significantly impact measurement accuracy. How to suppress the noise floor of the detection signal is one of the crucial means to enhance the measurement precision.

In a typical TDLAS gas sensor, the light beam is often converted into a parallel light with the use of a collimating lens and then focused onto a photo detector with a focusing lens. If the light beams reflected from the surfaces of these optical components enter the laser, an interference noise will be introduced into the signals output when the wavelength of the laser is modulated with a saw-tooth wave current. In order to reduce the interference noise, the anti-reflection coatings are applied onto these optical components[3]. Webster et al. introduced vibrating Brewster windows into optical systems to reduce interference fringes[4]. Persson et al. demonstrated

that balanced detection methods can effectively suppress interference fringes as well[5]. Although these techniques can be employed to reduce interference fringes, the potentially increase costs will be increased, and the sensor system becomes more complicated. Recently, the rapid development of machine learning technologies has provided more solutions for improving signal processing. Pang et al. demonstrated that a Back propagation neural network (BPNN) can effectively reduce interference fringe noise in a TDLAS system[6]. However, this method is prone to getting trapped in a local optimum, leading to suboptimal results. Although such approaches avoid adding complexity to sensor systems, the requirements of high demand power for chips also lead to significant challenges in practical applications. In engineering applications, digital signal filtering techniques remain main stream. Wang et al. proposed an improved model based on CEEMDAN-WTD to enhance detection accuracy to 0.65%[7]. While these methods have been proven effective in suppressing interference fringes, in certain cases, especially when gas concentrations are low, gas absorption spectra are often overshadowed by low-frequency, high-intensity interference fringes. The random variation in interference fringe phases complicates gas concentration measurements[8].

To address the issue of significant errors caused by interference noise floor generated by the laser itself, especially the impact of low-frequency, high-intensity interference fringes in harsh environmental engineering conditions, this paper reports a signal processing scheme that is capable of suppressing noise floor in detection signals during gas concentration measurements.

2. THEORY

2.1. TDLAS

It is well-known that the TDLAS technology is based on the infrared characteristic absorption of gas molecules. When a laser beam with a wavelength of λ (nm) passes through a gas, the absorb line of the gas will absorption the optical energy at the same wavelength. The change in optical intensity at a photo detector satisfies the Beer-Lambert Law:

$$I_t(v) = I_0(v)\exp\left[-\alpha(v)CL\right] \quad (1)$$

where, I_t denotes the intensity of the light after absorption, I_0 represents the initial light intensity, C stands for the volume fraction of the gas under measurement, L signifies the effective absorption path length, and $\alpha(v)$ indicates the absorption coefficient at the wavelength(λ). Hence, under conditions of stable pressure, temperature, and other factors, by computing the relative attenuation of light intensity, the amount of absorbed light energy for the gas under measurement at that wavelength can be derived, thus the actual gas concentration can be calculated. Therefore, TDLAS technology essentially constitutes a linear measurement process for detecting and processing analog signals. However, in TDLAS systems, various interference noise signals introduced from reflections on different optical component surfaces can impact measurement accuracy. This interference effect is particularly pronounced when gas concentrations are low, as the gas absorption spectra are often obscured by low-frequency, high-intensity background noise. Additionally, the random variation of interference fringe phases with environmental temperature renders precise measurement of low gas concentrations challenging.

2.2. Mechanism of Interference Fringe Generation

In conventional gas sensing systems based on absorption spectroscopy techniques, various types of lasers such as Distributed Feedback (DFB) lasers, Vertical-Cavity Surface-Emitting Lasers (VCSEL), Quantum Cascade Lasers (QCL), or inter-band Cascade Lasers (ICL) are utilized. These lasers are preferred for their narrow line widths, tenable, and ability to precisely tune the output wavelength to scan individual gas absorption lines. This facilitates high-sensitivity gas concentration detection using TDLAS technology. However, it is precisely due to the narrow line widths of the laser beams, the long coherence lengths of these laser beams will introduce interference if there are light reflected into the laser resonator cavity, especially when the coherence length far exceeds twice the length of the gas absorption cell, that any reflection from the reflective surfaces within the absorption cell back into the laser resonator cavity, under the influence of the laser wavelength scan tuned by the drive current, there will be interference fringes in the output beam of the laser, result in an interference noise at the output signal form the system.

As illustrated in Figure 1, in gas sensors based on TDLAS measurement technology, the laser requires a collimating lens to collimate the divergent laser beam into a parallel beam. This beam then passes through the sensing chamber and is converged onto the photosensitive surface of the detector by a converging lens, where the light energy is gathered. Hence, whenever a light beam reflected from the surface of a lens or the photosensitive surface of the detector enters the laser cavity after reflection and exits the laser outlet, interference occurs within the laser resonator cavity. Due to the different positions of the reflecting surfaces along the optical path, the spatial frequency of the interference fringes, or the size of the fringes, varies accordingly. For interferometer with smaller cavity lengths, larger interference fringes (low-frequency, high-intensity interference fringes) are produced, whereas for interferometers with larger cavity lengths, smaller interference fringes (high-frequency, low-intensity interference fringes) are generated. If the laser wavelength is tuned by the driving current while multiple interferometers coexist in the optical path, various interference fringes will superimpose in the photo detector and the interference noise appears in the detected optical signal. This results in the formation of interference noise in the detection signal, as depicted in Figure 1.

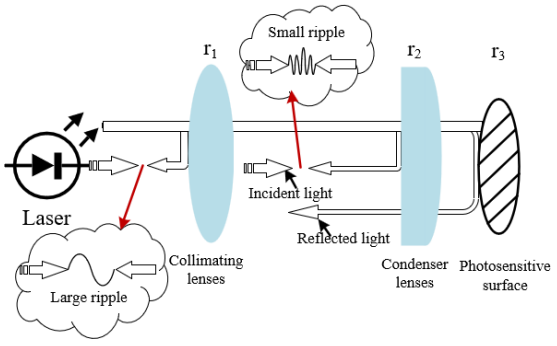

Figure 1. Generation of interference noise floor

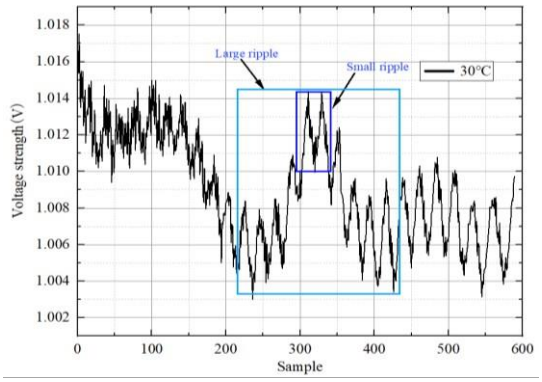

Figure 2. Interference signal at 0°C conditions

As shown depicted in Figure 2, the interference signal contains two types of interference fringe patterns, namely low-frequency, high-intensity interference fringes, or "large ripples" and high-frequency, low-intensity interference fringes or and "small ripples". The different fringe types are generated by the different interferences between the light emitted by the laser and the reflected light at different surfaces of optical lenses in the system. The position where the reflection occurs can be determined using Equation (2):

$$L = \frac{k}{2}\left(\frac{\lambda_1 \times \lambda_2}{\lambda_2 - \lambda_1}\right) \quad (2)$$

Where L represents the cavity length, k is the number of interference fringes within the sampling range, λ_1 is the starting wavelength of the scan, and λ_2 is the ending wavelength of the scan. By calculating the coherence length, two types of interference cavity lengths are identified: "large ripples" and "small ripples". By comparing the cavity lengths within the optical system, the "large ripples" interference primarily occurs between the laser resonator cavity and the inter-surface of the collimating lens, while the "small ripples" are produced between the laser resonator cavity and the surface of the photo detector. The primary factor affecting our detection accuracy is the low-frequency, high-intensity interference fringes generated between the laser resonator cavity and the inter-surface collimating lens, i.e. large ripples.

As depicted in Figure.3, when the laser is driven by a saw-tooth wave current, the large ripples directly superimpose on the absorption spectrum signal, introducing a non-linear enhancement in the signal strength of the zero baseline. This affects the accurate measurement of the baseline reference value, reducing the measurement accuracy when the low concentration methane is measured. Meanwhile, since the phase of interference fringes varies with changes in environmental temperature, the baseline of the signal will change accordingly. By comparing zero baseline signals at different temperatures, it can be seen in Figure 3, that this interference fringe phase changes cause the fluctuations of the signal baseline. Consequently, the irregular variation in signal intensity with temperature during the gas concentration measurements further increases the difficulty of high-precision detection. Hence, this paper proposes an algorithm to reduce the "large ripples" superimposed on the detection signal, thereby enhancing detection accuracy.

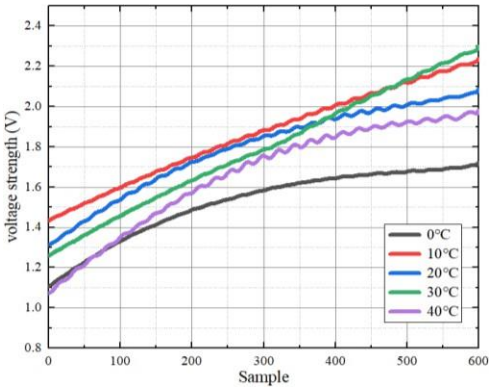

Figure 3. Detection signals at zero concentration for different temperatures

3. NEW SIGNAL PROCESSING METHOD

In order to reduce the measurement errors introduced by the larger ripples, a new signal processing method was used. In this method, the measured base line of the signal is extracted from each scanned signal, which is then compared with the theoretic baseline, resulting in the corresponding larger ripple baseline for each scan signal. Then by subtracting the corresponding larger ripple baseline from the original signal, the signal variations due to the corresponding larger ripple baseline are removed. Because the process of removing larger ripples is taken at the temperature when the measurement is made, as a result, the effect of the temperature induced base line variations is reduced. The steps used to process the signal are as the following:

1. To subtract the DC-bias caused by the photo detector and the detection circuit from the raw data measured in the experiment. The DC-bias of the photo detector at each scanning measurement is present in the detection signal obtained by the detector in each wavelength scanning cycle, and the corresponding DC-bias value is removed to obtain the raw detection signal.
2. To measure the temperature of the laser and the gas chamber respectively. The laser temperature is used to ensure that the center of the laser's wavelength scanning range coincides with the centerline of the Gaussian gas absorption spectrum of the methane gas, while the temperature of the sensor gas chamber is used to compensate for temperature-induced variations in the measured value.
3. In each scan cycle, subtract the starting signal value I_0 of the first sample point from the detector signals of 600 sample points respectively, and then, divide the detector signals of the 600 sampling points by the ending signal value I_{600} of the last sample point to obtain normalized data.
4. Use the detector signals of the first 100 sample points and those of the last 100 sample points from the normalized data, do a quadratic polynomial fit, and then subtract the ideal baseline from the quadratic polynomial fit data to obtain the ripple difference. The ideal baseline can be represented by Equation (3).

$$I_{idea} = \frac{1}{600} X \quad (3)$$

Where X represents the sample point, and I_{idea}

denotes the corresponding theoretic baseline value. The ideal detection baseline is obtained by multiplying the termination signal value I_{600} by the formula 3.

5. Subtract the ripple difference from the normalized data obtained in step 3 to obtain the signal data that are free from ripple interference.
6. Divide the idea baseline, I_{idea}, by the processed detection signal, *I*, which is free from ripple interference to obtain the absorbance ratio I_{idea}/I. Then, perform a *LN* transformation to get the processed measurement data.
7. Find the highest point or peak value and the position of its sampling point in the processed measurement data, which is located around the center of the wavelength scanning range or at the centerline of the Gaussian-shaped gas absorption spectrum. Integrate the processed measurement data over a range of 50 sampling points to the left and right of the peak value to obtain the measured value of the gas concentration. This method is designed to eliminate the uncertainty in the location of the highest point due to small ripples fluctuations, and to achieve the goal of improving the accuracy of the data.
8. The linear relationship between the measured value and the standard gas can be obtained by the calibration with the use of the standard gas. When the sensor is energized with different concentrations of the measured gas at different concentrations, the calibrated linear relationship can be then used to invert the measurement values to the corresponding concentration values.

4. EXPERIMENT

4.1. Experimental Setup

In order to verify if this algorithm can improve gas detection stability, an experiment set up as shown in Figure 4 was used. the temperature of the module is changed when a constant gas concentration is applied to the module, the tested results can be used to assess the measurement dispersion of gas concentration. The testing gas used in this experiment is carbon monoxide.

In can be seen from Figure 4, the outlet of the gas cylinder (Fig 4①) is connected to the inlet of a calibration nozzle (Fig 4②) that is placed onto the inlet of a CO module (Fig 4③), both the calibration nozzle and the module are placed in a temperature test chamber (Fig 4④). In the experiment, the CO module with the new algorithm firmware is placed inside the temperature test chamber. The calibration nozzle is securely fixed onto the outlet of the CO module. Then, the CO module is connected a communication module (Fig 4⑤) to enable online monitoring and debugging with the use of a computer(Fig 4⑥). The experimental setup is illustrated in the Figure 4.

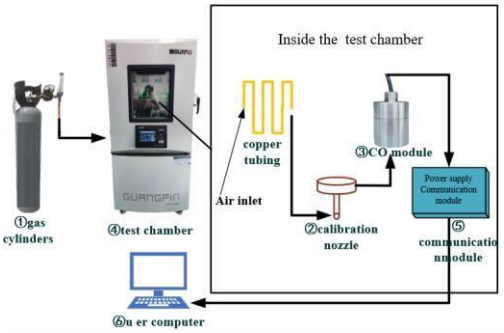

Figure 4. Diagram of the experimental setup

Using a control User interface in the computer, the temperature of the TEC inside the CO module is set to be 30°C for the laser in the module. A saw tooth driving current is applied to the laser to tuning the laser wavelength, so that the scanning range of the laser output wavelength covers the absorption spectrum of carbon monoxide. When the laser is at its set temperature, the center point of its wavelength scanning range aligns with the gas absorption spectrum line.

In order to check the temperature caused variation in the measurement, the experiment is carried out: Apply the gas concentration of 19.7 ppm onto the CO sensor, and allow ventilation for two minutes before the measurement and record data. The temperature of the test chamber is set at 0°C, 10°C, 20°C, 30°C, 40°C respectively. Wait for the temperature inside the test chamber to reach the preset temperature and stabilize. A two-minute socking time is applied between every two different temperature measurements. For every gas concentration, the measurements are repeated ten times.

4.2. Experimental Results

Figure 5 and Figure 6 show the comparison between the measured results before and after the optimization of the test data for the concentration of 19.7ppm at different temperatures.

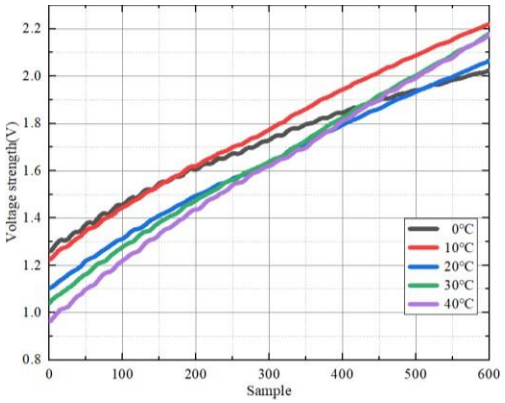

Figure 5. Detection signals at different temperatures

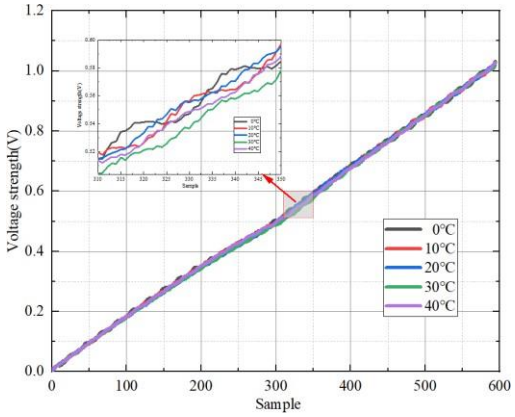

Figure 6. Detection signals at different temperatures after optimization

The noticeable improvement in the linearity of the detection signals at different temperatures after algorithm optimization suggests that the new algorithm effectively suppresses the non-linear enhancement of detection signal intensity caused by the irregular variation of interference fringes with temperature, Hence, this new algorithm enhances the stability of gas concentration detection.

With the use of this new algorithm to the CO module, the improvement of the gas detection stability can be verified. The results are presented in Figure 7.

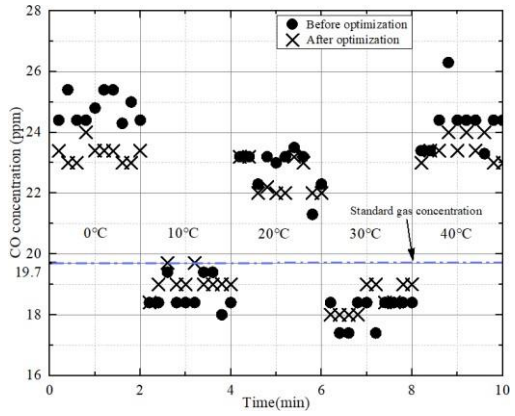

Figure 7. Comparison of Gas Concentrations before and after the Optimization

In Figure 7, the detected concentration values of 19.7 ppm under different ambient temperatures before and after the optimization using the new algorithm are shown. A comparison reveals that the concentration values (shown as “X” in Figure 7) obtained after the optimization are closer to those of the actual concentration. The calculated standard deviation before and after the optimization are 2.88 and 2.18 respectively. By comparing these values, it can be seen that the dispersion of the concentration values decreases by approximately 24.3% after the optimization. Hence, the new algorithm exhibits a mitigating effect on the irregular changes in interference fringes caused by variations in ambient temperature, leading to an improvement in the stability of CO concentration measurement.

5. CONCLUSION

The paper presents a signal processing scheme aimed at suppressing noise floor in the detection signals arising from laser interference variations during the gas concentration measurements, particularly targeting the mitigation of "large ripples" caused by the inference between the laser outlet and the surface of the collimating lens. The new algorithm was experimentally validated with the use of the experimental setup. The experimental results demonstrate that after processing with this new algorithm, the measured CO gas concentrations at different ambient temperatures are closer to the actual concentrations. The dispersion of the concentration values are decreased by 24.3%. This enhancement indicates an improvement in both the stability and accuracy of gas detection. Additionally, this algorithm exclusively targets the interference noise generated by the laser itself, and it can be combined with other algorithms designed to suppress additional interference fringes to enhance the capabilities of the measurement system on noise suppression. Preliminary results indicate that this new algorithm has potential for interference suppression in TDLAS systems and could be applied to methane, carbon dioxide, and other gas detection systems in the future.

ACKNOWLEDGMENTS

This work was supported by Shandong Micro-sensor Photonics Co. Ltd (91370100768729253k) and National Key Research Development Program of China (2022YFB3207602).

FUNDING STATEMENT

This work was supported by Shandong Micro-sensor Photonics Co. Ltd (91370100768729253k) and National Key Research the Development Program of China (2022YFB3207602).

REFERENCES

[1] Li Ma, Li Zou, Li-Feng Ren, Yi-Hong Chung, Peng-Yu Zhang, Chi-Min Shu. Prediction indices and limiting parameters of coal spontaneous combustion in the Huainan mining area in China[J]. Fuel, 2020, 264: 116883.

[2] J. Y. Li, L. H. Li, S. Zhao, P. Ren, S. J. Tian, H. L. Jin, Application research of tunable diode laser absorption spectroscopy in petroleum industry, Laser Optoelectron. P. 59 (13) (2022) 1300006, https://doi.org/10.3788/LOP202259.1300006.

[3] Ahlberg, H., Lundqvist, S., Shumate, M. S., & Persson, U. (1985). Analysis of errors caused by optical interference effects in wavelength-diverse CO 2 laser long-path systems. *Applied optics*, *24*(22), 3917-3923.

[4] C.R. Webster, Brewster-plate spoiler: a novel method for reducing the amplitude of interference fringes that limit tunable-laser absorption sensitivities, J. Opt. Soc. Am. B: Opt. Phys. 2 (9) (1985) 1464–1470.

[5] Persson, L., Andersson, F., Andersson, M., & Svanberg, S. (2007). Approach to optical interference fringes reduction in diode laser absorption spectroscopy. *Applied Physics B*, *87*, 523-530.

[6] Dongdong Pang, Lei Li, Lin Ma, Zhaohan Lin, Peng Liu, Xin Zhou, Interference fringe suppression in tunable diode laser

absorption spectroscopy based on BPNN, Optics Communications, Volume 544,2023,129630, ISSN 0030-4018

[7] Wang, S., Gong, W., Wang, Z., Wei, Y., Li, Y., Zhang, T., ... & Liu, T. (2022). Interference fringe suppression in tunable diode laser absorption spectroscopy based on CEEMDAN-WTD. *Frontiers in Physics*, *10*, 1057519.

[8] Reid, J., Shewchun, J., Garside, B. K., & Ballik, E. A. (1978). High sensitivity pollution detection employing tunable diode lasers. *Applied Optics*, *17*(2), 300-307.